Available online at www.sciencedirect.com
ScienceDirect
European Journal of Mechanics B/Fluids 26 (2007) 93–104

A numerical investigation of the steady evaporation of a polyatomic gas

Aldo Frezzotti

Dipartimento di Matematica, Politecnico di Milano, Piazza Leonardo da Vinci, 32, 20133 Milano, Italy

Received 12 October 2005; received in revised form 11 March 2006; accepted 14 March 2006

Available online 4 August 2006

Abstract

The evaporation and condensation of a polyatomic vapor in contact with its condensed phase has received much less attention than the monatomic case. In this paper we investigate the structure of the Knudsen layer formed in the steady evaporation of a vapor whose molecules behave as rigid rotators. The vapor motion is obtained by the numerical solution of the Boltzmann equation by the Direct Simulation Monte Carlo (DSMC) method. The obtained results are also compared with the solutions of a simplified kinetic BGK-like model equation. It is shown that density and temperature drops across the Knudsen layer are reasonably well reproduced by approximate methods proposed in the literature.

Keywords: Kinetic theory; Evaporation; Polyatomic gases; Monte Carlo

1. Introduction

In many situations, both of theoretical and practical interest, it is required to model the transfer of mass, momentum and energy between the vapor phase and its condensed phase (liquid or solid) coexisting in the same flowfield. Although hydrodynamic equations (Euler or Navier–Stokes) generally provide an adequate description of flow properties far from the vapor–liquid or vapor–solid interface, it is well known that there exists a narrow region (Knudsen layer) where the mechanical interaction between the vapor and the condensed phase is to be treated by the microscopic approach of the kinetic theory of gases [1]. The Knudsen layer formed during evaporation or condensation processes is only a few mean free paths wide, but the macroscopic quantities appearing in hydrodynamic equations may suffer strong jumps across this kinetic region. The necessity of describing the structure of the Knudsen layer and providing jump relationships to be used as boundary conditions for a hydrodynamic treatment of multi-phase flows has triggered the production of a huge number of papers where the problem has been extensively investigated [2]. However, most of the research activity has been concentrated on studying monatomic substances whereas evaporation or condensation of a polyatomic vapor in contact with its condensed phase has not attracted the same attention, in spite of their importance for many applications [3]. A paper by Cercignani [4] is the first reference which covers the whole range of admissible downstream Mach number values and provides relatively simple jump formulas which can be used to match the Knudsen layer to a hydrodynamic region which might exist in the flowfield [3]. In Ref. [4], the

E-mail address: aldo.frezzotti@polimi.it (A. Frezzotti).

0997-7546/$ – see front matter
doi:10.1016/j.euromechflu.2006.03.007

steady one-dimensional evaporation of a polyatomic gas possessing j internal indistinguishable degrees of freedom is studied by a BGK-like kinetic model equation [5,6] solved by an extension of the method of moments used by Ytrehus [7] for a monatomic gas. A more accurate solution method has been proposed by Soga [8] to study weak evaporation and condensation of a polyatomic gas by the linearized version of a similar kinetic model equation. Further approximate methods have been proposed by Skovorodko [9] and Zharov et al. [10] to correct some inaccuracies which were noted in Cercignani's results when the downstream Mach number approached the sonic limit. With the exception of the study of a linearized model equation described in Ref. [8], investigations quoted above are based on strongly simplified solution methods in order to obtain closed form jump relationships. Since the accuracy of these approximate methods does not seem to have been assessed yet, the work described in the present paper simply aims at presenting an investigation of the steady evaporation of a polyatomic gas by solving numerically both a model kinetic equation and the full Boltzmann equation for a vapor composed of classical rigid rotators. The adopted numerical methods, finite differences for the model kinetic equation and Direct Simulation Monte Carlo (DSMC) [11] for the Boltzmann equation, are free from the limitations of moment methods and allow us to obtain accurate solutions which can then be used as benchmarks.

2. Statement of the problem

We consider the steady one-dimensional flow of a polyatomic vapor evaporating from an infinite planar surface (interface) kept at constant and uniform temperature T_w. The surface, located at $x = 0$, separates the condensed phase, which occupies the half-space $x < 0$, from the vapor phase flowing in the half-space $x > 0$. The coordinate x spans the direction normal to the surface in a reference frame at rest with respect to the interface. The validity of the results obtained from the one-dimensional flow geometry also extends to problems in which the vapor–liquid/solid interface is not planar but its curvature radius is much larger than the reference mean free path. In this case, the kinetic region can be locally treated as one-dimensional. The problem treatment presented here is limited to the temperature range where vibrational excitation can be neglected. Moreover, since the gap between quantized rotational energy levels is supposed to be much smaller than κT_w, vapor molecules are supposed to behave as classical rigid rotators of *average* diameter a and mass m with $j = 2$ (linear molecule) or $j = 3$ (non-linear molecule) rotational degrees of freedom. Accordingly, the vapor motion in the positive half-space is assumed to be governed by the steady form of the following one-dimensional kinetic equation [1]:

$$\frac{\partial f}{\partial t} + v_x \frac{\partial f}{\partial x} = I(f, f) \tag{1}$$

where $f(\boldsymbol{v}, \epsilon|x, t)$ is the distribution function of molecular velocity $\boldsymbol{v}$ and rotational energy ϵ at location x and time t. The term $I(f, f)$, whose specific forms are given below, represents the collisional rate of change of f. It should be noted that rotational degrees of freedom are described by the rotational energy ϵ, not by the angular momentum vector $\boldsymbol{I}$ since no preferential alignment of molecular spinning motion is possible in the present problem.

The flowfield structure in the condensed phase has not been calculated. Molecular exchange processes between the vapor and condensed phase across the interface have been described by the following boundary condition for f at $x = 0$:

$$v_x f(\boldsymbol{v}, \epsilon|0, t) = v_x f_e(\boldsymbol{v}, \epsilon) + \int\limits_{v_{1x}<0} K(\boldsymbol{v}, \epsilon|\boldsymbol{v}_1, \epsilon_1)|v_{1x}| f(\boldsymbol{v}_1, \epsilon_1|0, t)\, \mathrm{d}\boldsymbol{v}_1\, \mathrm{d}\epsilon_1, \quad v_x > 0. \tag{2}$$

The distribution function of evaporating molecules, f_e, is assumed to be a half-range Maxwellian:

$$f_e(\boldsymbol{v}, \epsilon) = \sigma_e \frac{N_w}{(2\pi RT_w)^{3/2}} \exp\left(-\frac{\boldsymbol{v}^2}{2RT_w}\right) \frac{\epsilon^{j/2-1}}{\Gamma(j/2)(\kappa T_w)^{j/2}} \exp\left(-\frac{\epsilon}{\kappa T_w}\right), \quad v_x > 0. \tag{3}$$

The velocities of vapor molecules re-emitted into the gas phase after interacting with the interface are obtained by the following scattering kernel K which describes a pure diffusive re-emission [1]:

$$K(\boldsymbol{v}, \epsilon|\boldsymbol{v}_1, \epsilon_1) = (1 - \sigma_e) \frac{1}{2\pi(RT_w)^2} \exp\left(-\frac{\boldsymbol{v}^2}{2RT_w}\right) \frac{\epsilon^{j/2-1}}{\Gamma(j/2)(\kappa T_w)^{j/2}} \exp\left(-\frac{\epsilon}{\kappa T_w}\right). \tag{4}$$

In Eqs. (3), (4) N_w denotes the saturated vapor density at temperature T_w, σ_e is the evaporation coefficient, κ is the Boltzmann constant, R denotes the ratio κ/m and Γ is the complete Gamma function. It is further assumed that the far downstream vapor state is described by an equilibrium Maxwellian distribution function:

$$f_\infty(\boldsymbol{v},\epsilon) = \frac{N_\infty}{(2\pi RT_\infty)^{3/2}} \exp\left[-\frac{(\boldsymbol{v}-\boldsymbol{u}_\infty)^2}{2RT_\infty}\right] \frac{\epsilon^{j/2-1}}{\Gamma(j/2)(\kappa T_\infty)^{j/2}} \exp\left(-\frac{\epsilon}{\kappa T_\infty}\right) \tag{5}$$

with number density N_∞, temperature T_∞ and mean velocity $\boldsymbol{u}_\infty = u_\infty \hat{\boldsymbol{x}}$, being $\hat{\boldsymbol{x}}$ a unit vector normal to the interface. Normalizing x to the reference mean free path $\lambda_w = 1/(\sqrt{2}\pi N_w a^2)$, $\boldsymbol{v}$ to $\sqrt{RT_w}$ and ϵ to κT_w easily shows that the problem solutions, for fixed gas properties, depend on the following three parameters: N_∞/N_w, T_∞/T_w, $M_\infty = u_\infty/\sqrt{\gamma RT_\infty}$, γ being the specific heat ratio $c_p/c_v = (5+j)/(3+j)$. It has been shown [2] that, in the case of a monatomic gas ($j = 0$), the following general properties hold for steady solutions of Eq. (1):

- Only *subsonic* steady evaporation flows are possible, $0 \leqslant M_\infty < 1$.
- If purely diffusive reemission at $x = 0$ is present, then the vapor mean velocity has to be normal to the interface
- Two out of the three parameters listed above depend on the third one. Therefore, for example, one may write

$$\frac{N_\infty}{N_w} = \frac{N_\infty}{N_w}(M_\infty), \tag{6}$$

$$\frac{T_\infty}{T_w} = \frac{T_\infty}{T_w}(M_\infty). \tag{7}$$

The important relationships ((6) and (7)) give the jumps of macroscopic flow properties across the Knudsen layer and provide boundary conditions for the hydrodynamic description of the flowfield outside the Knudsen layers separating the regions occupied by the vapor from those occupied by the condensed phase. Although there is no reason to doubt that the general features outlined above would still hold for a polyatomic gas, the particular form of the jump formulas is affected by rotational degrees of freedom, as shown in previous studies.

3. Collision models

Two different expressions of the collision term $I(f, f)$ have been used to study the problem described above. The first and simpler expression is based on Holway's model [12] which approximates the collision term by the following BGK-like expression [5]:

$$\nu_{\rm el}(n, T_t)(\Phi_{\rm el} - f) + \nu_{\rm in}(n, T_t)(\Phi_{\rm in} - f) \tag{8}$$

where the "frozen" local equilibrium and local equilibrium Maxwellian distribution functions, $\Phi_{\rm el}(\boldsymbol{v},\epsilon)$ and $\Phi_{\rm in}(\boldsymbol{v},\epsilon)$, are defined as follows:

$$\Phi_{\rm el}(\boldsymbol{v},\epsilon) = \frac{n(\epsilon|x,t)}{[2\pi RT_t(x,t)]^{3/2}} \exp\left\{-\frac{[\boldsymbol{v}-\boldsymbol{u}(x,t)]^2}{2RT_t(x,t)}\right\}, \tag{9}$$

$$\Phi_{\rm in}(\boldsymbol{v},\epsilon) = \frac{N(x,t)}{[2\pi RT(x,t)]^{3/2}} \exp\left\{-\frac{[\boldsymbol{v}-\boldsymbol{u}(x,t)]^2}{2RT(x,t)}\right\} \frac{\epsilon^{j/2-1}}{\Gamma(j/2)[\kappa T(x,t)]^{j/2}} \exp\left[-\frac{\epsilon}{\kappa T(x,t)}\right]. \tag{10}$$

The first term describes elastic collisions, whereas the second one models inelastic collisions. The macroscopic fields associated with $\Phi_{\rm el}(\boldsymbol{v},\epsilon)$ and $\Phi_{\rm in}(\boldsymbol{v},\epsilon)$ are defined as:

$$n(\epsilon|x,t) = \int f(\boldsymbol{v},\epsilon|x,t)\,\mathrm{d}^3v, \tag{11}$$

$$N(x,t) = \int f(\boldsymbol{v},\epsilon|x,t)\,\mathrm{d}^3v\,\mathrm{d}\epsilon = \int n(\epsilon|x,t)\,\mathrm{d}\epsilon, \tag{12}$$

$$\boldsymbol{u}(x,t) = \frac{1}{N(x,t)} \int \boldsymbol{v} f(\boldsymbol{v},\epsilon|x,t)\,\mathrm{d}^3v\,\mathrm{d}\epsilon = u_x(x,t)\hat{\boldsymbol{x}}, \tag{13}$$

$$T_t(x,t) = \frac{1}{3RN(x,t)} \int \left[\boldsymbol{v}-\boldsymbol{u}(x,t)\right]^2 f(\boldsymbol{v},\epsilon|x,t)\,\mathrm{d}^3v\,\mathrm{d}\epsilon, \tag{14}$$

$$T_r(x,t) = \frac{2}{j\kappa N(x,t)} \int \epsilon f(\boldsymbol{v}, \epsilon|x,t)\, \mathrm{d}^3 v\, \mathrm{d}\epsilon, \tag{15}$$

$$T(x,t) = \frac{3T_t(x,t) + jT_r(x,t)}{3+j}. \tag{16}$$

The quantity $n(\epsilon|x,t)$ is the number density of molecules having rotational energy ϵ, $N(x,t)$ is the total number density, $\boldsymbol{u}(x,t)$ is the mean velocity of the gas, whereas $T_t(x,t)$, $T_r(x,t)$ and $T(x,t)$ are the translational, rotational and overall temperature, respectively. The elastic and inelastic collision frequencies, $\nu_{\mathrm{el}}(n,T_t)$ and $\nu_{\mathrm{in}}(n,T_t)$ have been computed from the shear viscosity μ_{hs} of the hard sphere gas as:

$$\nu_{\mathrm{el}}(N,T_t) = (1-z)\nu_{\mathrm{tot}}(N,T_t), \tag{17}$$

$$\nu_{\mathrm{in}}(N,T_t) = z\nu_{\mathrm{tot}}(N,T_t), \tag{18}$$

$$\nu_{\mathrm{tot}}(N,T_t) = \frac{N\kappa T_t}{\mu_{\mathrm{hs}}(T_t)}, \tag{19}$$

$$\mu_{\mathrm{hs}}(T_t) = \frac{5}{16}\frac{\sqrt{\pi m \kappa T_t}}{\pi a^2}. \tag{20}$$

In Eqs. (17), (18) $1-z$ and z are the fractions of elastic and inelastic number of collisions. The model parameter z, which tunes the strength of translational-rotational coupling, has been set equal to a constant, although it could be a function of the temperature.

The numerical solution of Eq. (1) with the collision term (8) can be greatly simplified by a transformation first considered by Chu [13]. Let us define the reduced distribution functions $F(v_x|x,t)$, $G(v_x|x,t)$ and $H(v_x|x,t)$ as:

$$\begin{pmatrix} F(v_x|x,t) \\ G(v_x|x,t) \\ H(v_x|x,t) \end{pmatrix} = \int \begin{pmatrix} 1 \\ v_y^2 + v_z^2 \\ \epsilon \end{pmatrix} f(\boldsymbol{v}, \epsilon|x,t)\, \mathrm{d}v_y\, \mathrm{d}v_z\, \mathrm{d}\epsilon. \tag{21}$$

It can be easily verified that the reduced distribution functions defined above obey the following system of kinetic equations:

$$\frac{\partial}{\partial t}\begin{pmatrix} F \\ G \\ H \end{pmatrix} + v_x \frac{\partial}{\partial x}\begin{pmatrix} F \\ G \\ H \end{pmatrix} = \nu_{\mathrm{el}}\begin{pmatrix} \widehat{F}_{\mathrm{el}} - F \\ \widehat{G}_{\mathrm{el}} - G \\ \widehat{H}_{\mathrm{el}} - H \end{pmatrix} + \nu_{\mathrm{in}}\begin{pmatrix} \widehat{F}_{\mathrm{in}} - F \\ \widehat{G}_{\mathrm{in}} - G \\ \widehat{H}_{\mathrm{in}} - H \end{pmatrix} \tag{22}$$

where

$$\begin{pmatrix} \widehat{F}_{\mathrm{el}}(v_x|x,t) \\ \widehat{G}_{\mathrm{el}}(v_x|x,t) \\ \widehat{H}_{\mathrm{el}}(v_x|x,t) \end{pmatrix} = \begin{pmatrix} 1 \\ 2RT_t(x,t) \\ \frac{j\kappa T_r}{2} \end{pmatrix} \frac{N(x,t)}{\sqrt{2\pi RT_t}} \exp\left\{-\frac{(v_x-u_x)^2}{2RT_t}\right\}, \tag{23}$$

$$\begin{pmatrix} \widehat{F}_{\mathrm{in}}(v_x|x,t) \\ \widehat{G}_{\mathrm{in}}(v_x|x,t) \\ \widehat{H}_{\mathrm{in}}(v_x|x,t) \end{pmatrix} = \begin{pmatrix} 1 \\ 2RT(x,t) \\ \frac{j\kappa T(x,t)}{2} \end{pmatrix} \frac{N(x,t)}{\sqrt{2\pi RT}} \exp\left\{-\frac{(v_x-u_x)^2}{2RT}\right\}. \tag{24}$$

Boundary conditions for the reduced distribution functions at $x=0$ are easily derived from Eqs. (2)–(4).

Although the interest in the numerical solutions of a kinetic model equation is justified by the necessity of assessing the quality of previous studies, a further comparison with a more sophisticated collision model is desirable. A particle scheme has then been adopted to solve the Boltzmann equation for a polyatomic gas whose collision dynamics and cross-section have been obtained from a phenomenological model proposed by Borgnakke and Larsen [14]. The model overcomes some of the restrictions and complications of previous mechanical models of translational-rotational coupling (rough spheres, loaded spheres, spherocylinders) [15] since it can be easily adapted to reproduce experimental translational-rotational relaxation rates with good accuracy [16]. Moreover, the collision algorithm derived from the model is very well suited to particle schemes used to obtain numerical solutions of the Boltzmann equation [11].

A dilute gas of classical rigid rotators undergoing binary collisions can be described by a kinetic equation having the following general form [17]:

$$\frac{\partial f}{\partial t} + v_x \frac{\partial f}{\partial x} = \int \left[f\left(\boldsymbol{v}_1', \epsilon_1'|x\right) f\left(\boldsymbol{v}', \epsilon'|x\right) - f(\boldsymbol{v}_1, \epsilon_1|x) f(\boldsymbol{v}, \epsilon|x) \right] Q \epsilon_1^{\mu}\, \mathrm{d}^3 v_1\, \mathrm{d}\epsilon_1. \tag{25}$$

In Eq. (25), Q is defined as

$$Q = \int_{\mathcal{S}} \mathrm{d}^2\hat{\boldsymbol{e}}' \int_0^{E-\epsilon'} \epsilon'^{\mu}\,\mathrm{d}\epsilon' \int_0^{E-\epsilon_1'} \epsilon_1'^{\mu}\,\mathrm{d}\epsilon_1' \frac{v_r'^2}{v_r}\sigma\left(E;\hat{\boldsymbol{e}}'\circ\hat{\boldsymbol{e}};\epsilon',\epsilon_1'\to\epsilon,\epsilon_1\right) \tag{26}$$

being $\sigma(E;\hat{\boldsymbol{e}}'\circ\hat{\boldsymbol{e}};\epsilon',\epsilon_1'\to\epsilon,\epsilon_1)$ the differential cross-section associated with a binary collision which produces a pair of molecules in the final states $(\boldsymbol{v},\epsilon)$, $(\boldsymbol{v}_1,\epsilon_1)$ from a pair of molecules in the initial states $(\boldsymbol{v}',\epsilon')$, $(\boldsymbol{v}_1',\epsilon_1')$. The argument E denotes the conserved total energy in the center of mass reference frame:

$$E = \frac{1}{4}mv_r^2 + \epsilon + \epsilon_1 = \frac{1}{4}mv_r'^2 + \epsilon' + \epsilon_1'. \tag{27}$$

The unit vectors $\hat{\boldsymbol{e}}' = \boldsymbol{v}_r'/v_r'$ and $\hat{\boldsymbol{e}} = \boldsymbol{v}_r/v_r$ have the directions of the relative velocities $\boldsymbol{v}_r' = \boldsymbol{v}_1' - \boldsymbol{v}'$ and $\boldsymbol{v}_r = \boldsymbol{v}_1 - \boldsymbol{v}$ before and after a collision, respectively. The exponent μ in Eq. (25) takes the values 0 for $j = 2$ and $\frac{1}{2}$ for $j = 3$.

In the particular form of the Borgnakke–Larsen model adopted here, collision dynamics is organized as follows:

- The collision probability of two molecules in the pre-collision states $(\boldsymbol{v}',\epsilon')$, $(\boldsymbol{v}_1',\epsilon_1')$ is proportional to $\sigma_{\mathrm{hs}}v_r'$, where $\sigma_{\mathrm{hs}} = \pi a^2$ is the integral cross-section of hard sphere molecules and $v_r' = \|\boldsymbol{v}_1' - \boldsymbol{v}'\|$ is the relative velocity modulus.
- An individual collision is inelastic with probability z or elastic with probability $1 - z$. An inelastic collision gives rise to an exchange between translational and rotational energies, as explained below. In an elastic collision pre- and post-collision rotational energies do not change, i.e. $\epsilon = \epsilon'$, $\epsilon_1 = \epsilon_1'$. Conservation of total energy then implies $v_r = v_r'$ and, according to hard sphere impact dynamics, post-collision relative velocity is written as $\boldsymbol{v}_r = v_r\hat{\boldsymbol{e}}$, being $\hat{\boldsymbol{e}}$ a random vector uniformly distributed on the unit sphere $\mathcal{S}$.
- In an inelastic collision total energy E is randomly partitioned between translational and rotational motion by sampling the translational energy fraction E_{tr}/E from a given probability density function $\mathcal{P}_1(E_{\mathrm{tr}}/E|j)$. The available total rotational energy $E_{\mathrm{rot}} = \epsilon + \epsilon_1 = E - E_{\mathrm{tr}}$ is then randomly distributed between the collision partners by sampling the fraction $\epsilon/E_{\mathrm{rot}}$ from a given probability density function $\mathcal{P}_2(\epsilon/E_{\mathrm{rot}}|j)$. The relative velocity after a collision is again written as $\boldsymbol{v}_r = v_r\hat{\boldsymbol{e}}$, where $\hat{\boldsymbol{e}}$ is a random unit vector and $v_r = \sqrt{4E_{\mathrm{tr}}/m}$.

The specific form of the probability densities $\mathcal{P}_1(\epsilon/E_{\mathrm{rot}}|j)$ and $\mathcal{P}_2(E_{\mathrm{tr}}/E|j)$ depends both on the number of internal degrees of freedom and on the assumed intermolecular interaction [11]. In the case of hard sphere interaction and $j = 2$ they take a particularly simple form [11,17]:

$$\mathcal{P}_1(E_{\mathrm{tr}}/E|2) = 6\frac{E_{\mathrm{tr}}}{E}\left(1 - \frac{E_{\mathrm{tr}}}{E}\right), \tag{28}$$

$$\mathcal{P}_2(\epsilon/E_{\mathrm{rot}}|2) = 1. \tag{29}$$

As shown by Eq. (28), post-collision translational energy has a parabolic distribution; the available E_{rot} amount is then randomly divided between ϵ and ϵ_1, according to Eq. (29). Taking into account the assumed scattering isotropy and Eqs. (28), (29), the collision cross-section takes the form:

$$\sigma\left(E;\hat{\boldsymbol{e}}'\circ\hat{\boldsymbol{e}};\epsilon',\epsilon_1'\to\epsilon,\epsilon_1\right) = \frac{\sigma_{\mathrm{hs}}}{4\pi E^2}\theta\left(\mathcal{E},\mathcal{E}_1,\mathcal{E}',\mathcal{E}_1'\right), \tag{30}$$

$$\theta\left(\mathcal{E},\mathcal{E}_1,\mathcal{E}',\mathcal{E}_1'\right) = (1-z)\delta\left(\mathcal{E}-\mathcal{E}'\right)\delta\left(\mathcal{E}_1-\mathcal{E}_1'\right) + 6z(1-\mathcal{E}-\mathcal{E}_1) \tag{31}$$

being $\mathcal{E} = \epsilon/E$.

The strength of translational-rotational coupling is determined by the mixing parameter z which can be made to depend on the local flowfield temperature to fit experimental relaxation rates [16].

4. Description and discussion of numerical results

Steady solutions of the kinetic equations described in the previous section have been obtained as the long time limit of unsteady solutions in the finite spatial domain

$$D_x = \{x \in \mathcal{R}:\ 0 < x < L\}$$

bounded by the condensed phase at $x = 0$ and by an imaginary plane located at position $x = L$, far enough from the interface to avoid distortions in the flowfield.

Since the Knudsen layer thickness is a monotonically increasing function of M_∞, the extent L of the spatial domain has been varied from $20\lambda_\infty$ to $250\lambda_\infty$ while varying the downstream Mach number from about 0.1 to about 0.97. Numerical solutions of Holway's kinetic model have been obtained by the simple technique described in Ref. [18]. The finite interval $[0, L]$, which replaces the half-space $x > 0$, has been divided into $\mathcal{N}_x$ cells of variable size, smaller spatial cells being associated with the region of stronger gradients. Each reduced distribution function has been assumed to be constant within a spatial cell. A similar representation has been adopted for the one-dimensional reduced velocity space which has been replaced by a finite interval $D_v = \{v_x \in \mathcal{R}\colon\ v_{\min} < v_x < v_{\max}\}$ whose bounds have to be set wide enough to contain the significant part of the distribution functions. The interval D_v has been divided into $\mathcal{N}_v$ equally spaced cells whose typical size did not exceed $0.02\sqrt{RT_w}$. A simple first order upwind scheme has been used to approximate the advection term in Eqs. (22) and an implicit scheme has been used to advance the distribution functions values from one time level to the next, till the onset of steady flow condition.

The Boltzmann equation has been solved by a variant of Direct Simulation Monte Carlo (DSMC) method proposed by Koura [19]. In this case the distribution function f is represented by $\mathcal{N}_p$ particles moving through a spatial grid and colliding according to the rules described above. Because of the intrinsic statistical nature of the numerical method, macroscopic quantities are obtained by time averaging particle properties over a long time interval after the decay of the initial transient. Not less than 50 particles per spatial cell have been used in each simulation and the various computational parameters (grid size, time step, time averaging duration...) have been carefully tuned to ensure a good accuracy level.

The application of both techniques to the present problem is straightforward. However, it is worth mentioning that the boundary condition at infinity given by Eq. (5) requires some attention since not all the parameters of the upstream equilibrium state can be freely specified in a steady subsonic solution, as shown by Eqs. (6), (7). Actually, the relationship among the problem parameters is the main outcome of the calculations and it is not known beforehand. Therefore, the distribution function of molecules entering the computational domain from the boundary at $x = L$ is not completely specified. The problem, common to both numerical methods, can be solved by adopting a milder boundary condition which only forces the distribution function to be symmetric with respect to a specified velocity value u_∞. The Maxwellian equilibrium state with correct values of N_∞ and T_∞ is then automatically produced by the system evolution [20].

The same boundary condition has been implemented in two different ways in the deterministic solution of Eqs. (22) and in the DSMC solution of Eq. (25). In the first case, the distribution function of molecules entering the computational domain from the boundary at $x = L$ is obtained by requiring that, for $v_x < 0$, the following conditions hold

$$F(v_x|L,t) = F(v_x^*|L,t), \tag{32}$$

$$G(v_x|L,t) = G(v_x^*|L,t), \tag{33}$$

$$H(v_x|L,t) = H(v_x^*|L,t) \tag{34}$$

where $v_x^* = 2u_\infty - v_x$ is the velocity value symmetric to v_x with respect to u_∞. When solving the Boltzmann equation by DSMC, the boundary condition at $x = L$ can be equivalently formulated as described below. Again, the downstream vapor velocity u_∞ is the only fixed parameter and the distribution function at $x = L$ is forced to be symmetric with respect to u_∞:

$$f(\boldsymbol{v}^*, \epsilon|L,t) = f(\boldsymbol{v}, \epsilon|L,t), \tag{35}$$

$$\boldsymbol{v}^* = 2u_\infty \hat{\boldsymbol{x}} - \boldsymbol{v}. \tag{36}$$

The boundary condition (35) is easily translated into a simple algorithm which updates the particles velocities without any reference to a specific shape of f. Whenever a particle in D_x crosses the plane $x = L$, its velocity $\boldsymbol{v}$ is changed to $\boldsymbol{v}^*$ according to Eq. (36). If the x component of $\boldsymbol{v}^*$, v_x^*, is less than zero then the particle is allowed to reenter the domain with a probability p given by the following expression:

$$p = \frac{|v_x^*|}{v_x}. \tag{37}$$

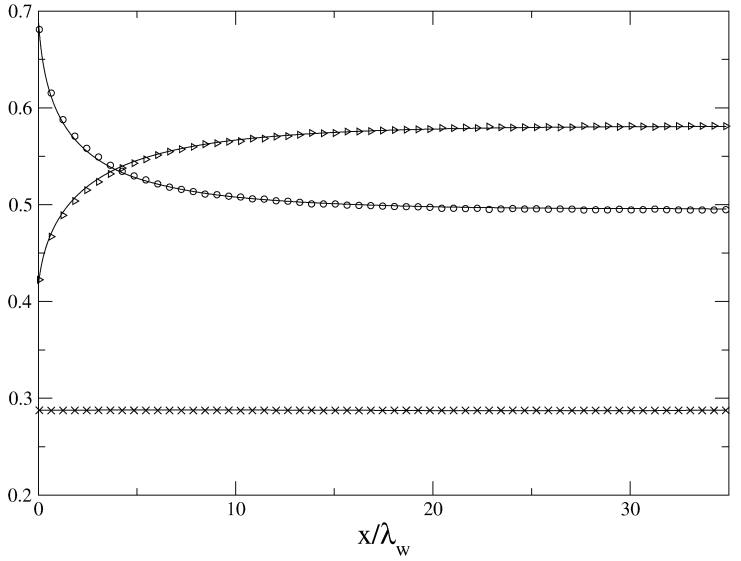

Fig. 1. Density, velocity and mass flux profiles in evaporation flow of a polyatomic gas with $j = 3$ rotational degrees of freedom; $z = 0.3$, $M_\infty = 0.534$. Numerical data from solution of Holway's kinetic model are represented by solid lines. DSMC results represented by symbols: ∘, $N(x)/N_w$; ▷, $u_x(x)/\sqrt{RT_w}$; ×, $J(x) = N(x)u_x(x)/N_w\sqrt{RT_w}$.

Eq. (37) is easily derived taking into account that the flux ϕ^+ of particles with velocity $\boldsymbol{v}$ and rotational energy ϵ crossing the rightmost boundary is $\phi^+ = f(\boldsymbol{v}, \epsilon|L, t)v_x$, $(v_x > 0)$, whereas the flux ϕ^- of particles with velocity $\boldsymbol{v}^*$ and rotational energy ϵ reentering the domain with $v_x^* < 0$ is $\phi^- = f(\boldsymbol{v}^*, \epsilon|L, t)v_x^*$. The ratio $|\phi^-|/\phi^+$ is equal to p and does not involve f because of the symmetry condition (35).

Solutions presented here have been obtained by varying the computational parameters of both numerical methods (grid size, particles number) until no appreciable changes were caused by further refinements. The downstream Mach number M_∞ has been varied form zero to about 0.97. Obtaining solutions with almost sonic downstream state requires a considerable amount of computing time because of the increasing Knudsen layer thickness [7] and the slower rate of convergence to the steady state. As shown below, the highest value of M_∞ considered here is close enough to the sonic limit to judge about the quality of previous studies. In most of the numerical calculations presented here the parameter z has been set equal to 0.3. The chosen value is not specific for a particular substance and it simply appears to be reasonable for low temperature flows of diatomic gases like nitrogen [16]. It should be observed that the particular choice of z does not appear to be crucial to obtain Eqs. (6), (7) since the strength of translational-rotational coupling does affect the local structure of the Knudsen layer but it seems to have no effects on the jump relationships [8]. In all cases presented here the evaporation coefficient has been set equal to 1.0 to follow the choice made in previous investigations.

4.1. Knudsen layer structure

The typical structure of the non-equilibrium flow within the Knudsen layer is shown in Figs. 1 and 2, where density, velocity, mass flux and temperature profiles are presented for a vapor with $j = 3$. The downstream Mach number M_∞ is 0.534, whereas z has been set equal to 0.3. The first figure shows a steady expansion flow with a monotonically decreasing density and a monotonically increasing mean velocity. Both quantities reach their limit values, N_∞ and u_∞, approximately at a distance of 30 reference mean free paths λ_w. It is worth noting that the computed mass flux profile is extremely close to a constant function, as required by a steady one-dimensional flow.

The thickness of the Knudsen layer is an increasing function of M_∞ [7] and grows up to about $250\lambda_w$ in the numerical solutions with the highest downstream Mach number. The non-equilibrium state of the flowfield is best appreciated from the examination of temperature profiles shown in Fig. 2. In the vicinity of the interface, the different velocity distributions of molecules with positive and negative component v_x produce a strong anisotropy of f in the

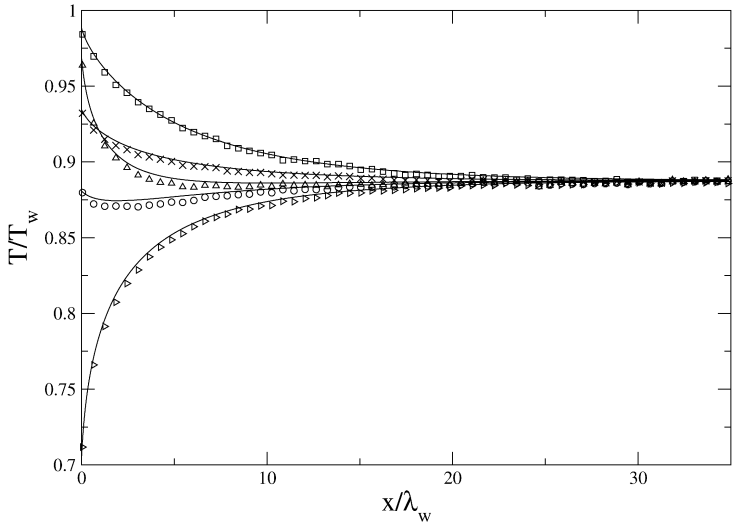

Fig. 2. Temperature profiles in evaporation flow of a polyatomic gas with $j = 3$ rotational degrees of freedom; $z = 0.3$, $M_\infty = 0.534$. Numerical data from solution of Holway's kinetic model are represented by solid lines. DSMC results represented by symbols: ∘, $T_t(x)/T_w$; ▷, $T_\parallel(x)/T_w$; △, $T_\perp(x)/T_w$; □, $T_r(x)/T_w$; ×, $T(x)/T_w$.

velocity space and remarkable differences between parallel temperature $T_\parallel(x)$, transversal temperature $T_\perp(x)$ and translational temperature $T_t(x)$ defined as

$$T_\parallel(x) = \frac{1}{N(x)R}\int \big[v_x - u_x(x)\big]^2 f(\boldsymbol{v}, \epsilon|x)\,\mathrm{d}^3 v\,\mathrm{d}\epsilon, \tag{38}$$

$$T_\perp(x) = \frac{1}{2N(x)R}\int \big(v_y^2 + v_z^2\big) f(\boldsymbol{v}, \epsilon|x)\,\mathrm{d}^3 v\,\mathrm{d}\epsilon, \tag{39}$$

$$T_t(x) = \frac{T_\parallel(x) + 2T_\perp(x)}{3}. \tag{40}$$

The rotational temperature is not affected by the anisotropy in the velocity space, therefore T_r is closer to T_w than translational temperature, in the vicinity of the interface.

It should be noticed that the overall temperature $T(x)$ is a monotonically decreasing function whereas the translational temperature exhibits a slight minimum. The behavior of $T_t(x)$ can be easily explained since the vapor expansion initially causes a translational temperature drop which is later compensated by the energy exchange with rotational degrees of freedom which finally cause $T_t(x)$ to increase toward the common limit value T_∞. The behavior of the translational temperature profile is strongly affected by the strength of translational-rotational coupling and the minimum can be turned into a maximum by increasing z. The effect is shown in Fig. 3 which presents temperature profiles computed from Holway's kinetic model. The downstream Mach number is the same as in Fig. 2, but z has been increased to 1.0, its maximum value. Now the coupling is strong enough to overcome the effect of the expansion which can cause a decrease in $T_t(x)$ only when the difference $T_r(x) - T_t(x)$ is somewhat reduced. It should be observed that, as discussed below in greater detail, changing z does affect temperature relaxation and the structure of the Knudsen layer in general, but not the downstream equilibrium state. It is also interesting to note that non-monotonic temperature profiles exhibiting a local maximum are reported in Ref. [10] where the strong evaporation of a polyatomic gas is studied by a moment method. However, no clear distinction between translational and rotational temperature seems to have been made both in the *Ansatz* for the distribution function and in the model which appears to have been formulated in terms of an overall gas temperature $T(x)$. In the present calculations $T(x)$ is always a monotonically decreasing function.

Figs. 1 and 2 also compare Boltzmann equation results with those obtained from the kinetic model. In complete analogy with the monatomic case [20], the two approaches produce very close profiles of macroscopic quantities and, within the precision of numerical calculations, identical downstream equilibrium values, thus adding further evidence that jump formulas are not sensitive to the details of the molecular collision model [8,20,21].

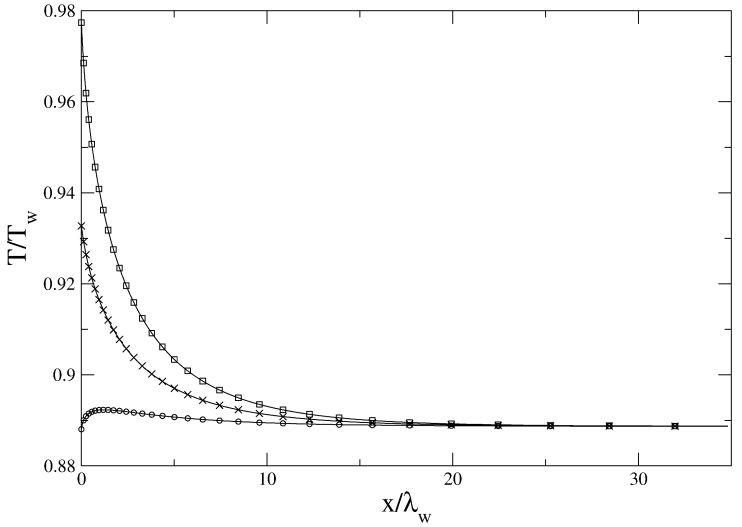

Fig. 3. Numerical solution of Holway's kinetic model. Temperature profiles in evaporation flow of a polyatomic gas with $j = 3$ rotational degrees of freedom; $z = 1.0$, $M_\infty = 0.534$. ∘, $T_t(x)/T_w$; □, $T_r(x)/T_w$; ×, $T(x)/T_w$.

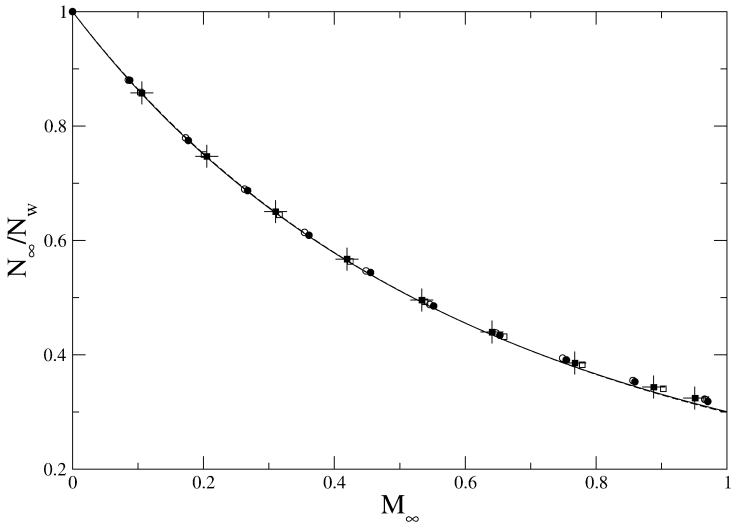

Fig. 4. Normalized downstream density as a function of M_∞. Moment method, Ref. [4]: solid line, $j = 2$; dashed line, $j = 3$. DSMC solution of Boltzmann equation: ∘, $j = 2$, $z = 0.3$; □, $j = 3$, $z = 0.3$. Numerical solution of Holway's model kinetic equation: •, $j = 2$, $z = 0.3$; ■, $j = 3$, $z = 0.3$; +, $j = 3$, $z = 1.0$.

4.2. Jump relationships

Numerical values of downstream normalized density and temperature as functions of M_∞ are given in Figs. 4 and 5 for $j = 2$ and $j = 3$. The values of the density ratio N_∞/N_w computed from Eq. (25) are in excellent agreement with those obtained from the numerical solution of the kinetic model equation and with the moment method results described in Ref. [4]. As observed in previous studies, the density ratio appears to be almost insensitive to the presence of rotational degrees of freedom. Moreover, values obtained from different translational-rotational coupling constants seem to collapse onto a single curve.

The temperature ratio T_∞/T_w exhibits greater sensitivity to the number of rotational degrees of freedom which reduce the temperature drop caused by the vapor expansion, as shown in Fig. 5. Again, the values T_∞/T_w computed from Eq. (25) are in excellent agreement with those obtained from the kinetic model but it is observed a significant

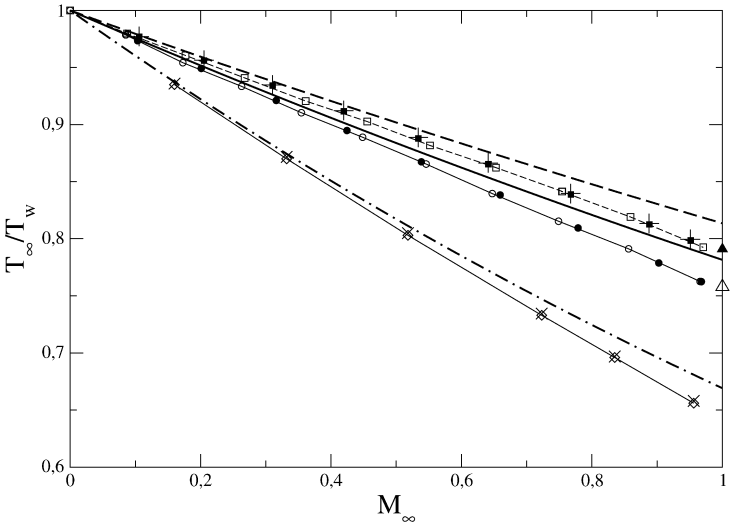

Fig. 5. Normalized downstream temperature as a function of M_∞. Moment method, Ref. [4]: dotted-dashed line, monatomic gas, $j = 0$; solid line, $j = 2$; dashed line, $j = 3$. DSMC solution of Boltzmann equation: $\diamond$, monatomic gas, $j = 0$ (from Ref. [20]); $\circ$, $j = 2$, $z = 0.3$; $\square$, $j = 3$, $z = 0.3$. Numerical solution of Holway's model kinetic equation: $\bullet$, $j = 2$, $z = 0.3$; $\blacksquare$, $j = 3$, $z = 0.3$; $+$, $j = 3$, $z = 1.0$; $\times$, monatomic gas, $j = 0$ (BGK model results from Ref. [20]). Sonic limit values, Ref. [9]: $\triangle$, $j = 2$; $\blacktriangle$, $j = 3$.

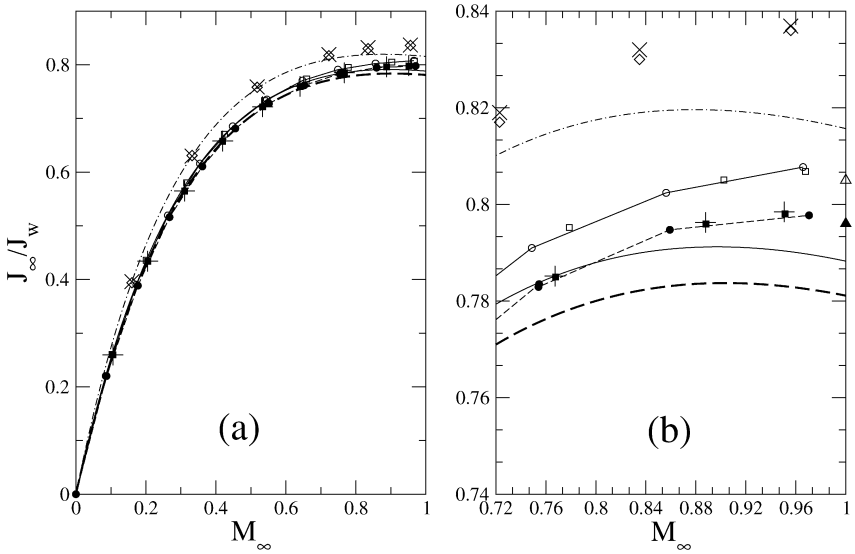

Fig. 6. Graph (a) – normalized mass flux as a function of M_∞. Moment method, Ref. [4]: dotted-dashed line, monatomic gas, $j = 0$; solid line, $j = 2$; dashed line, $j = 3$. DSMC solution of Boltzmann equation: $\diamondsuit$, monatomic gas, $j = 0$ (from Ref. [20]); $\circ$, $j = 2$, $z = 0.3$; $\square$, $j = 3$, $z = 0.3$. Numerical solution of Holway's model kinetic equation: $\bullet$, $j = 2$, $z = 0.3$; $\blacksquare$, $j = 3$, $z = 0.3$; $+$, $j = 3$, $z = 1.0$; $\times$, monatomic gas, $j = 0$, (BGK model results from Ref. [20]). Graph (b) – Enlarged view of high Mach number region of graph (a). Line marking is the same as in graph (a). Sonic limit values, Ref. [9]: $\triangle$, $j = 2$; $\blacktriangle$, $j = 3$.

deviation from moment method which predicts smaller drops both for $j = 2$ and $j = 3$. The discrepancy does not appear to be peculiar to the moment method extension to polyatomic gases since the same behavior is also present in the monatomic case ($j = 0$), as shown in Fig. 5 where moment method data are represented by the dotted-dashed line whereas the results of DSMC and BGK simulations from Ref. [20] are represented by diamonds and crosses, respectively.

The T_∞/T_w curves reported in Refs. [9,10] seem to be in better agreement with the present numerical calculations. Skovorodko's predictions for T_∞/T_w at sonic downstream condition are 0.758 for $j = 2$ and 0.791 for $j = 3$. Both

values are only slightly above sonic values that could be extrapolated from DSMC or Holway's model data given in Fig. 5.

Although obtainable from data presented above, the net mass flux $J_\infty = N_\infty u_\infty$ deserves some attention because it is a flow property of fundamental importance. Fig. 6 compares the values of the mass flux predicted by the moment method [4] with the present results. In both figures, mass flux values are normalized to $J_w = N_w\sqrt{RT_w/(2\pi)}$ which represents the maximum mass flux intensity,in absence of back scatter. All methods predict a slight decrease of the net mass flux at fixed M_∞ when j increases, the effect being more evident at high Mach numbers. The difference between the results from the numerical solution of kinetic equations and moment method predictions are rather small and particularly evident only in the vicinity of sonic downstream conditions. In general, moment method seems to overestimate the fraction of back scattered molecules,thus giving a lower net mass flux for all values of j considered here. The mass flux is a monotonically increasing function of M_∞. However, as observed in Ref. [9], the approximate expression for J_∞/J_w derived in Ref. [4] predicts the occurrence of an unphysical local maximum before the sonic condition is achieved. As shown in Fig. 7, the maximum is not pronounced and it is not peculiar to the moment method extension to polyatomic gases, since it is also present for $j = 0$ when the method reduces to Ytrehus's tri-modal *Ansatz*. The approximate jump formulas described in Ref. [9] produce the correct qualitative behavior of J_∞/J_w and the reported limit values at $M_\infty = 1$ seem pretty close to a reasonable extrapolation of the present numerical results to sonic condition, both for $j = 2$ and $j = 3$.

5. Conclusions

As stated in the introductory section, the aim of the present work is to present a numerical approach to the study of steady evaporation of a polyatomic gas into a half-space. The Knudsen layer structure and numerical value of jump formulas have been obtained by solving the Boltzmann equation and a kinetic model equation. The numerical results have been used to assess the accuracy of previous investigations which were based on strongly simplified methods. The results show that, in general, approximated jump formulas proposed in the literature perform well and provide values close to the present results. In particular, the simple method proposed in Ref. [9] seems effective in correcting the deficiencies observed in the earlier application of the moment method.

References

[1] C. Cercignani, The Boltzmann Equation and Its Applications, Springer-Verlag, Berlin, 1988.
[2] Y. Sone, Kinetic theoretical studies of the half-space problem of evaporation and condensation, TTSP 29 (3–5) (2000) 227–260.
[3] A.V. Rodionov, J.F. Crifo, K. Szego, J. Lagerros, M. Fulle, An advanced physical model of cometary activity, Planetary and Space Science 50 (2002) 983–1024.
[4] C. Cercignani, Strong evaporation of a polyatomic gas, in: Rarefied gas Dynamics; International Symposium, 12th, Charlottesville, VA, July 7–11, 1980, Technical Papers. Part 1, American Institute of Aeronautics and Astronautics, New York, 1981, pp. 305–320.
[5] P.L. Bhatnagar, E.P. Gross, M. Krook, A model for collision processes in gases. I. Small amplitude processes in charged and neutral one-component systems, Phys. Rev. 94 (1954) 511–525.
[6] T.F. Morse, Kinetic model for gases with internal degrees of freedom, Phys. Fluids 7 (1964) 159.
[7] T. Ytrehus, Theory and experiments on gas kinetics in evaporation, in: J.L. Potter (Ed.), Rarefied Gas Dynamics: Technical Papers Selected from the 10th International Symposium on Rarefied Gas Dynamics, Snowmass-at-Aspen, CO, July 1976, in: Progress in Astronautics and Aeronautics, vol. 51, American Institute of Aeronautics and Astronautics, 1977, p. 1197.
[8] T. Soga, A kinetic theory analysis of evaporation and condensation of a diatomic gas, Phys. Fluids 28 (1985) 1280–1285.
[9] P.A. Skovorodko, Semi-empirical boundary conditions for strong evaporation of a polyatomic gas, in: T. Bartel, M. Gallis (Eds.), Rarefied Gas Dynamics, 22th International Symposium, Sydney, Australia, 9–14 July 2000, in: AIP Conference Proceedings, vol. 585, American Institute of Physics, Melville, NY, 2001, pp. 588–590.
[10] N.A. Zharov, I.A. Kudnetsova, A.A. Yushkanov, Intense evaporation of molecular gas, High Temperature 36 (1998) 109–115.
[11] G.A. Bird, Molecular Gas Dynamics and the Direct Simulation of Gas Flows, Clarendon Press, Oxford, 1994.
[12] L.H. Holway, New statistical models for kinetic theory, Phys. Fluids 9 (1966) 1658–1673.
[13] C.K. Chu, Kinetic-theoretic description of the formation of a shock wave, Phys. Fluids 8 (1965) 12–22.
[14] C. Borgnakke, P.S. Larsen, Statistical collision model for Monte Carlo simulation of polyatomic gas mixtures, J. Comput. Phys. 18 (1975) 405–420.
[15] S. Chapman, T.G. Cowling, The Mathematical Theory of Non-Uniform Gases, Cambridge University Press, Cambridge UK, 1990.
[16] I.J. Wysong, D.C. Wadsworth, Assessment of direct simulation Monte Carlo phenomenological rotational relaxation models, Phys. Fluids 10 (1998) 2983–2994.
[17] I. Kuščer, A model for rotational energy exchange in polyatomic gases, Physica A 158 (1989) 784–800.

[18] A. Frezzotti, Numerical investigation of the strong evaporation of a polyatomic gas, in: A. Beylich (Ed.), Proceedings of the 17th International Symposium on Rarefied Gas Dynamics, Aachen, 1990, VCH Verlagsgesellschaft, Weinheim, 1991, pp. 1243–1250.
[19] K. Koura, Null-collision technique in the direct-simulation Monte Carlo method, Phys. Fluids 29 (1986) 3509–3511.
[20] A. Frezzotti, Kinetic theory description of the evaporation of multi-component substances, in: C. Shen (Ed.), Rarefied Gas Dynamics, Proceedings of the 20th International Symposium, Beijing, China, 19–23 August 1996, Peking University Press, Beijing, China, 1997, pp. 837–846.
[21] S.M. Yen, T.J. Akai, Nonlinear numerical solutions for an evaporation–effusion problem, in: J.L. Potter (Ed.), Rarefied Gas Dynamics: Technical Papers Selected from the 10th International Symposium on Rarefied Gas Dynamics, Snowmass-at-Aspen, CO, July 1976, in: Progress in Astronautics and Aeronautics, vol. 51, American Institute of Aeronautics and Astronautics, 1977, p. 1175.